

Original Article



Impairment of Mitochondrial ATP Synthesis Induces RIPK3-dependent Necroptosis in Lung Epithelial Cells During Lung Injury by Lung Inflammation

Su Hwan Lee ¹, Ju Hye Shin ¹, Min Woo Park ², Junhyung Kim ²,
Kyung Soo Chung ¹, Sungwon Na ³, Ji-Hwan Ryu ⁴, Jin Hwa Lee ⁵,
Moo Suk Park ¹, Young Sam Kim ^{1,*}, and Jong-Seok Moon ^{2,*}

OPEN ACCESS

Received: Oct 18, 2021

Revised: Mar 7, 2022

Accepted: Mar 30, 2022

Published online: Apr 15, 2022

***Correspondence to**

Young Sam Kim

Division of Pulmonary and Critical Care Medicine, Department of Internal Medicine, Severance Hospital, Yonsei University College of Medicine, 50-1 Yonsei-ro, Seodaemun-gu, Seoul 03722, Korea.

Email: ysamkim@yuhs.ac

Jong-Seok Moon

Department of Integrated Biomedical Science, Soonchunhyang Institute of Medi-bio Science (SIMS), Soonchunhyang University, 25 Bongjeong-ro, Dongnam-gu, Cheonan 31151, Korea.

Email: jongseok81@sch.ac.kr

Copyright © 2022. The Korean Association of Immunologists

This is an Open Access article distributed under the terms of the Creative Commons Attribution Non-Commercial License (<https://creativecommons.org/licenses/by-nc/4.0/>) which permits unrestricted non-commercial use, distribution, and reproduction in any medium, provided the original work is properly cited.

ORCID iDs

Su Hwan Lee

<https://orcid.org/0000-0002-3487-2574>

Ju Hye Shin

<https://orcid.org/0000-0003-1830-6828>

¹Division of Pulmonary and Critical Care Medicine, Department of Internal Medicine, Severance Hospital, Yonsei University College of Medicine, Seoul 03722, Korea

²Department of Integrated Biomedical Science, Soonchunhyang Institute of Medi-bio Science (SIMS), Soonchunhyang University, Cheonan 31151, Korea

³Department of Anesthesiology and Pain Medicine, Anesthesia and Pain Research Institute, Yonsei University College of Medicine, Seoul 03722, Korea


⁴Severance Biomedical Science Institute, Yonsei University College of Medicine, Seoul 03722, Korea


⁵Division of Pulmonary and Critical Care Medicine, Department of Internal Medicine, Ewha Womans University, College of Medicine, Seoul 07804, Korea

ABSTRACT

Dysfunction of mitochondrial metabolism is implicated in cellular injury and cell death. While mitochondrial dysfunction is associated with lung injury by lung inflammation, the mechanism by which the impairment of mitochondrial ATP synthesis regulates necroptosis during acute lung injury (ALI) by lung inflammation is unclear. Here, we showed that the impairment of mitochondrial ATP synthesis induces receptor interacting serine/threonine kinase 3 (RIPK3)-dependent necroptosis during lung injury by lung inflammation. We found that the impairment of mitochondrial ATP synthesis by oligomycin, an inhibitor of ATP synthase, resulted in increased lung injury and RIPK3 levels in lung tissues during lung inflammation by LPS in mice. The elevated RIPK3 and RIPK3 phosphorylation levels by oligomycin resulted in high mixed lineage kinase domain-like (MLKL) phosphorylation, the terminal molecule in necroptotic cell death pathway, in lung epithelial cells during lung inflammation. Moreover, the levels of protein in bronchoalveolar lavage fluid (BALF) were increased by the activation of necroptosis via oligomycin during lung inflammation. Furthermore, the levels of ATP5A, a catalytic subunit of the mitochondrial ATP synthase complex for ATP synthesis, were reduced in lung epithelial cells of lung tissues from patients with acute respiratory distress syndrome (ARDS), the most severe form of ALI. The levels of RIPK3, RIPK3 phosphorylation and MLKL phosphorylation were elevated in lung epithelial cells in patients with ARDS. Our results suggest that the impairment of mitochondrial ATP synthesis induces RIPK3-dependent necroptosis in lung epithelial cells during lung injury by lung inflammation.


Keywords: Mitochondrial dysfunction; Necroptosis; Lung inflammation; Acute lung injury


Min Woo Park 
<https://orcid.org/0000-0002-9616-2543>

 Junhyung Kim 
<https://orcid.org/0000-0002-5054-2700>

 Kyung Soo Chung 
<https://orcid.org/0000-0003-1604-8730>

 Sungwon Na 
<https://orcid.org/0000-0002-1170-8042>

 Ji-Hwan Ryu 
<https://orcid.org/0000-0001-6969-7465>

 Jin Hwa Lee 
<https://orcid.org/0000-0003-0843-9862>

 Moo Suk Park 
<https://orcid.org/0000-0003-0820-7615>

 Young Sam Kim 
<https://orcid.org/0000-0001-9656-8482>

 Jong-Seok Moon 
<https://orcid.org/0000-0002-2537-7854>

Conflict of Interest

The authors declare no potential conflicts of interest.

Abbreviations

ALI, acute lung injury; ARDS, acute respiratory distress syndrome; BALF, bronchoalveolar lavage fluid; DAMP, damage-associated molecular pattern; MLKL, mixed lineage kinase domain-like; mtROS, mitochondrial reactive oxygen species; RIPK, receptor-interacting serine/threonine kinase; SDS, sodium dodecyl sulphate; TBS-T, Tris-buffered saline containing 0.05% Tween-20.

Author Contributions

Conceptualization: Lee SH, Kim YS, Moon JS; Data curation: Lee SH, Shin JH, Kim YS, Moon JS; Formal analysis: Lee SH, Shin JH, Park MW, Kim JH, Chung KS, Na SW, Ryu JH, Lee JH, Park MS; Funding acquisition: Lee SH, Moon JS; Investigation: Lee SH, Shin JH, Park MW, Kim JH; Methodology: Chung KS, Na SW, Ryu JH, Lee JH, Park MS; Resources: Chung KS, Na SW, Ryu JH, Lee JH, Park MS; Writing - original draft: Lee SH, Kim YS, Moon JS; Writing - review & editing: Lee SH, Kim YS, Moon JS.

INTRODUCTION

Mitochondrial dysfunction has emerged as a critical signature in the pathogenesis of human disease (1). Mitochondrial dysfunction is caused by physical changes, such as swelling, and biochemical changes, such as impaired oxidative phosphorylation and ATP production, decline in mitochondrial membrane potential, increased production of mitochondrial reactive oxygen species (mtROS) (2,3). Mitochondrial dysfunction is linked to cellular injury and death in human diseases (1).

Acute lung injury (ALI) is caused by an uncontrolled systemic inflammatory response resulting from direct injury to the lung or indirect injury in the setting of a systemic process (4). The pathogenesis of ALI involves inflammatory injury to the alveolocapillary membrane and the accumulation of protein-rich pulmonary edema fluid in the airspaces which leads to the pulmonary infiltrates and hypoxemia (5). Inflammatory injury is associated with apoptosis of epithelial cells in ALI (6). Several inflammation pathways such as toll-like receptor 4 (TLR4) signaling pathway are involved in the activation of inflammation during ALI (7,8). Previous study showed that TNF- α -induced death signaling is linked to alveolar epithelial dysfunction and the early pathophysiology of ALI (9). As the most severe form of ALI, acute respiratory distress syndrome (ARDS) is a form of diffuse alveolar injury (10). Although lung inflammation and cell death are characterized in the pathogenesis of ALI or ARDS, the mechanisms of the development of ALI or ARDS are not fully understood.

Necroptosis is a programmed form of necrosis (11,12). Necroptosis is regulated by the formation of necrosome which is a protein complex consisting of receptor-interacting serine/threonine kinase (RIPK)1, RIPK3 and mixed lineage kinase domain-like (MLKL) (11,12). Necroptosis leads to rapid plasma membrane permeabilization and to the release of damage-associated molecular patterns (DAMPs) (13). As a key molecule of the activation of necroptosis, RIPK3 induces the phosphorylation of MLKL, the terminal molecule in necroptotic cell death pathway, which leads to lysis the cellular membrane (14). In our previous study, we found that mitochondrial dysfunction promotes the activation of necroptosis in human lung epithelial cells (15). However, the mechanisms for the activation of necroptosis during lung injury by lung inflammation remain unclear.

In our study, we showed that the impairment of mitochondrial ATP synthesis induces RIPK3-dependent necroptosis during lung injury by lung inflammation. Our results found that the impairment of mitochondrial ATP synthesis by oligomycin increases lung injury and RIPK3 and RIPK3 phosphorylation levels in lung tissues during lung inflammation in mice. The elevated RIPK3 levels by oligomycin resulted in high MLKL phosphorylation in lung tissues during lung inflammation. Moreover, the levels of protein in bronchoalveolar lavage fluid (BALF) were increased by the activation of necroptosis via oligomycin during lung inflammation. Furthermore, the levels of ATP5A were reduced in lung epithelial cells of patients with ARDS, the most severe form of ALI. The reduced ATP5A levels contributes to elevation of RIPK3, RIPK3 phosphorylation and MLKL phosphorylation levels in lung epithelial cells in patients with ARDS. Our results suggest that the impairment of mitochondrial ATP synthesis exacerbates RIPK3-dependent necroptosis during lung injury by lung inflammation.

MATERIALS AND METHODS

Human study

The human subject study was conducted in accordance with the Declaration of Helsinki. The protocol was approved by the Institutional Review Board. Seven human ARDS patient slides were obtained according to the protocol approved by the Institutional Review Board of Severance Hospital in Yonsei University (IRB approval No. 4-2019-0831) (**Supplementary Table 1**). Two ARDS lung tissues were obtained with consent from patients undergoing lung transplantation with ARDS (**Supplementary Table 1**). Patients were enrolled in a lung transplant patient cohort (IRB approval No. 4-2013-0770). Non-ARDS subjects (non-ARDS) were obtained from human-derived material bank (IRB approval No. 4-2019-0447). We analyzed patients with ARDS who received lung transplantation. Retrospectively, we reviewed 241 consecutive lung transplantation patients between October 2012 and July 2019. Among the 241 patients, we specifically examined 7 patients with ARDS and 2 non-ARDS subjects (**Supplementary Table 1**). The bilateral diffuse infiltration was evaluated by chest X-ray in patients with ARDS or non-ARDS subjects.

Animal study

The animal experiments were performed according to the Guide for the Care and Use of Laboratory Animals (National Research Council, Washington, D.C., USA), approved by the Yonsei University Health System Institutional Animal Care and Use Committee (approval number: 2018-0158). Male 8-wk-old C57BL/6 mice (Orient Bio Inc., Seongnam, Korea) were intratracheally administered LPS (5 µg/g) derived from *Escherichia coli* 0111:B4 (InvivoGen, San Diego, CA, USA) for lung injury, whereas control mice were treated with equal volume of PBS. In the groups with promotion of necroptosis, 24 h and 1 h before treatment with LPS or PBS, oligomycin (0.5 mg/kg; Sigma-Aldrich, St. Louis, MO, USA) was injected intraperitoneally. One day after LPS or PBS administration, the trachea was washed thrice with 0.9 mL of PBS through a tracheal catheter to obtain BALF and collect lung tissue.

Analysis of immunoblot

Human lung tissues and whole right lung tissues from the mice were used for the quantification of protein levels by immunoblot. Lung tissues and paraffin embedded tissue sections were homogenized in 1 mL of radioimmunoprecipitation assay buffer (50 mM Tris-HCl, 0.1% sodium dodecyl sulphate [SDS], 2 mM ethylenediaminetetraacetic acid, 150 mM NaCl, 1% sodium deoxycholate; 1% Triton X-100; pH 7.5) or Tissue Extraction Reagent I (FNN0071; Thermo Fisher Scientific, Waltham, MA, USA) with protease inhibitor cocktail and phosphatase inhibitor cocktail. The homogenate was incubated for 20 min on ice and then centrifuged at $14,000 \times g$ for 15 min at 4°C. The supernatant was collected and the same volume of 5 X SDS buffer was added to the supernatant. The mixture was then boiled for 5 min and stored at -80°C. Proteins were separated by SDS-polyacrylamide gel electrophoresis on 4%–5% Q-PAGE Tris-Glycine Novel Precast Gel (SMOBIO Technology, Hsinchu City, Taiwan) or NuPAGE 4%–12% Bis-Tris gels (Thermo Fisher Scientific). After electrophoresis, proteins were transferred to polyvinylidene difluoride membranes (Millipore, Billerica, MA, USA) or Protran nitrocellulose membranes (10600001; GE Healthcare Life Science, Pittsburgh, PA, USA) and blocked in 5% non-fat milk or 5% (w/v) BSA (9048-46-8; Santa Cruz Biotechnology, Dallas, TX, USA) in Tris-buffered saline containing 0.05% Tween-20 (TBS-T) (TBS [170-6435; Bio-Rad Laboratories, Hercules, CA, USA] and Tween-20 [170-6531; Bio-Rad Laboratories]) at 25°C for 1 h. The membranes were immunoblotted with primary Abs against RIPK3 for mouse (AHP1797; Bio-Rad Laboratories), RIPK3 for human (ab62344; Abcam,

Cambridge, UK), Phospho-RIPK3 (Thr231/Ser232) for mouse (ab222320; Abcam), Phospho-RIPK3 (Ser227) for human (ab209384; Abcam), Phospho-MLKL (Ser345) (ab196436; Abcam) for mouse, Phospho-MLKL (Ser358) (ab187091; Abcam) for human, MLKL (ab243142; Abcam) for mouse, MLKL (ab184718; Abcam) for human, Phospho-RIPK1 (Ser166) (#31122; Cell Signaling Technology, Danvers, MA, USA) for mouse, Phospho-RIPK1 (Ser166) (NBP3-06877; Novus, Littleton, CO, USA) for human, and β -actin (A5316; Sigma-Aldrich) overnight at 4°C and washed five times with TBS-T for 10 min each at room temperature. The membranes were then incubated with the HRP-conjugated secondary Ab (goat anti-rabbit IgG-HRP [sc-2004], goat anti-mouse IgG-HRP [sc-2005] and goat anti-rat IgG-HRP [sc-2006] from Santa Cruz Biotechnology) (1:2,000 dilution in TBS-T) at 37°C for 1 h and were washed five times with TBS-T for 10 min each at 25°C. The membranes were treated with SuperSignal West Pico Chemiluminescent Substrate (34078; Thermo Fisher Scientific) and immunoreactive bands were detected.

Histopathological examination and lung injury scoring

The left lung of each mouse was fixed by perfusion with formaldehyde before routine processing and paraffin embedding. Slide sections were stained with H&E for histological examination. At least 20 images with high-power fields (400 \times total magnification) from each slide were randomly selected due to the patchy nature of the injury and lung injury scores were calculated (16). In animal study, each group (Control, Oligomycin, LPS, or Oligomycin+LPS) have 5 mice. Lung injury score was calculated by 100 fields from each group. Each field was evaluated by five histological findings (A. Neutrophils in the alveolar space, B. Neutrophils in the interstitial space, C. Hyaline membranes, D. Proteinaceous debris filling the airspaces and E. Alveolar septal thickening) and was graded using a three-tiered schema summarized in **Supplementary Table 2**. In human study, we analyzed lung injury score with 20 random images with high-power fields from each slide. Lung injury score was calculated by 40 fields from 2 normal and 140 fields from 7 patients with ARDS, respectively. Human lung tissue slide sections were further stained for immunohistochemical analysis of anti-RIPK3 Ab (ab62344; Abcam) to confirm necroptosis. Immunohistochemistry was performed using the RIPK3 Ab with Dako Autostainer Link 48 platform (Dako, Glostrup, Denmark).

Analysis of immunofluorescence and immunohistochemistry

For immunofluorescence analysis, lung tissues were sectioned from paraffin embedded tissue blocks at a thickness of 4 μ m. Sections were permeabilized in 0.5% Triton-X (T8787; Sigma-Aldrich), blocked in CAS-Block™ Histochemical Rea-gent (008120; Thermo Fisher Scientific), and then stained with the following Abs: polyclonal rabbit anti-Phospho Ser358-MLKL Ab (1:100) for human (ab187091; Abcam), polyclonal rabbit anti-Phospho Ser345-MLKL Ab (1:100) for mouse (ab196436; Abcam), monoclonal mouse anti-E-cadherin Ab (1:100) (sc-21791; Santa Cruz Biotechnology). Sections were then incubated with goat anti-rabbit IgG (H+L) Alexa Fluor 488 (1:100) (A11008; Thermo Fisher Scientific), polyclonal rabbit anti-ATP5A1 Ab (1:100) (18023; Cell Signaling Technology), and goat anti-mouse IgG H&L Texas Red (1:100) (ab6787; Abcam) secondary Ab at 25°C for 2 h. Fluoroshield™ with DAPI (F6057; Sigma-Aldrich) was used for nuclear staining. Stained brain sections were analyzed by THUNDER Imager Tissue (Leica Microsystems Ltd., Wetzlar, Germany). DAPI-stained nuclei are shown in blue. Stained brain sections were quantified by LAS X image-processing software (Leica Microsystems Ltd.) and ImageJ software v1.52a (National Institutes of Health, Bethesda, MD, USA). For immunohistochemistry analysis, tissues were stained with an Ab against specific targets. The secondary Ab was biotinylated goat anti-

rabbit IgG (Vector Laboratories, Burlingame, CA, USA), and biotinylated rabbit anti-goat (Vector Laboratories). Subsequently, streptavidin peroxidase complex (Vector Laboratories) was biotinylated for 2 h at 25°C. After staining, slides were mounted by Eukitt® Quick-hardening mounting medium (03989; Sigma-Aldrich). Stained sections were analyzed by Olympus BX53M microscope (Olympus, Tokyo, Japan) and quantified by the Olympus Stream software and ImageJ software v1.52a (National Institutes of Health). To ensure objectivity, all measurements were performed with blinded conditions by 2 observers per experiment under identical conditions.

Analysis for quantification of protein levels and number of cells in BALF

The BALF was centrifuged (4°C, 400 ×g, 10 min) and the protein content was measured in the supernatant using Pierce BCA Protein Assay Kit (Thermo Fisher Scientific). After incubation for 30 min at 37°C, the plate was cooled, and the absorbance was read at 562 nm in a spectrophotometer. The cell pellet was reconstituted in 100 μL PBS and used to analyze the cells quantitatively and qualitatively. Total cell number in each sample was determined using a hemocytometer (Paul Marienfeld GmbH, Lauda-Königshofen, Germany) according to the manufacturer's protocol. An aliquot of each sample (90 μL) was transferred into the slide chambers and inserted into a cytopsin with the slide facing out-ward. The slides were centrifuged at 400 ×g for 6 min, and then removed and dried before staining. The slides were immersed in three DiffQuick fluids (Fixative, Solution I, and Solution II) and rinsed with purified water.

Statistical analysis

All data are represented as mean±SD or SEM. A 2-tailed Student's t-test for comparison of two groups, and ANOVA (with post hoc comparisons using Dunnett's test) for comparison of two or more groups were used for statistical analysis using GraphPad Prism version 5.01 (GraphPad Software Inc., San Diego, CA, USA). Additionally, the analysis of lung injury score in mouse and human lung samples was performed using the Kruskal-Wallis test or Mann-Whitney test in SPSS version 25 (IBM Corp., Armonk, NY, USA). In all comparisons, p-values were considered statistically significant.

RESULTS

Impairment of ATP synthesis exacerbates lung injury by lung inflammation

To investigate the role of impaired ATP synthesis in lung injury by lung inflammation, we analyzed whether the impairment of ATP synthesis by oligomycin, an inhibitor of ATP synthase, could exacerbate lung injury by lung inflammation in a model of ALI. We used a lung inflammation mouse model using LPS, a ligand of TLR4. To examine the effects of impaired ATP synthesis, we injected oligomycin to mice with LPS-induced lung inflammation. The lung injury scores were increased by LPS-induced lung inflammation in lung tissues of LPS alone (LPS) or oligomycin and LPS (Oligomycin + LPS) compared to that in mice with control (Control), whereas oligomycin alone (Oligomycin) did not change lung injury (**Fig. 1A and B**). Notably, the lung injury was significantly higher in Oligomycin + LPS than that in mice with LPS (**Fig. 1B**). Although the levels of TNF-α were increased by LPS-induced lung inflammation in BALF, Oligomycin + LPS did not change the levels of TNF-α compared to LPS (**Fig. 1C**). These results suggest that the impairment of ATP synthesis exacerbates lung injury by lung inflammation.

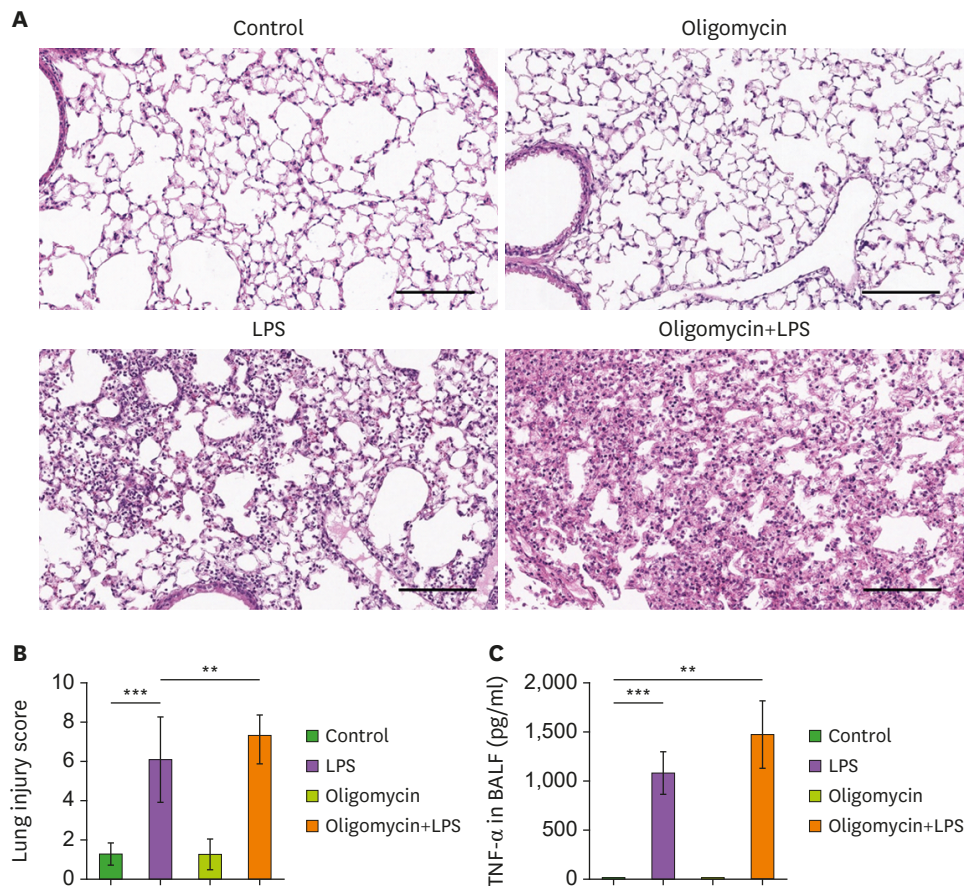


Figure 1. Impairment of ATP synthesis exacerbates lung injury by lung inflammation. (A) Representative images for H&E staining and (B) quantification of lung injury scores of lung tissues from mice treated with oligomycin either control or LPS. Scale bars, 200 μ m. Lung injury score was calculated by 100 fields from each group (n=20 images per individual subject, n=5 per each group). (C) Quantification of TNF- α levels in BALF from mice treated with oligomycin either control or LPS (n=5 per each group). Data are representative of three independent experiments. Data are mean \pm SD. **p<0.01; ***p<0.001 by Student's 2-tailed t-test, ANOVA or Kruskal-Wallis test.

Impairment of ATP synthesis increases the levels of RIPK3 in lung tissues during lung injury by lung inflammation

Next, we investigated molecular mechanism which by the impairment of ATP synthesis promotes lung injury by lung inflammation. We analyzed whether the impairment of ATP synthesis could induce RIPK3-mediated necroptosis during lung injury by lung inflammation. We measured the protein levels of RIPK3 in lung tissues from mice treated with oligomycin during LPS-induced lung inflammation. The levels of RIPK3 were increased by LPS in lung tissues of mice relative to that in Control (**Fig. 2A and B**). Notably, the levels of RIPK3 were significantly elevated by Oligomycin + LPS compared to that in mice with LPS (**Fig. 2A and B**). Consistently, the levels of RIPK3 phosphorylation (Thr231/Ser232) were elevated by Oligomycin + LPS compared to that in mice with LPS (**Fig. 2A and B**). Moreover, the levels of MLKL phosphorylation (Ser345) were elevated by Oligomycin + LPS compared to that in mice with LPS (**Fig. 2A and B**). The levels of RIPK1 phosphorylation (Ser166) were comparable between Oligomycin + LPS and LPS (**Fig. 2A and B**). These results suggest that the impairment of ATP synthesis increases the levels of RIPK3 in lung tissues during lung injury by lung inflammation.

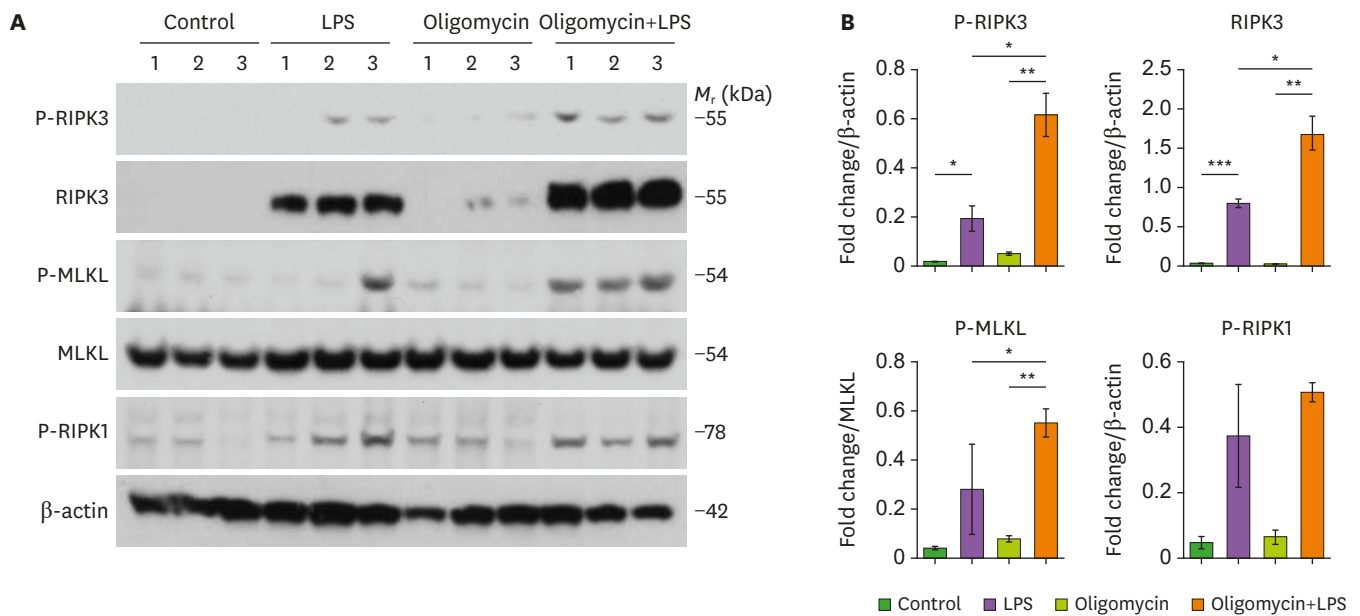


Figure 2. Impairment of ATP synthesis increases the levels of RIPK3 in lung tissues during lung injury by lung inflammation. (A) Representative immunoblot images of RIPK3 phosphorylation (Thr231/Ser232), RIPK3, MLKL phosphorylation (Ser345), MLKL, RIPK1 phosphorylation (Ser166) protein and (B) quantification of RIPK3 phosphorylation, RIPK3, MLKL phosphorylation, RIPK1 phosphorylation protein levels in lung tissues from mice treated with oligomycin either control or LPS (n=3 per each group). β -actin or MLKL were used as loading control. Data are representative of three independent experiments. Data are mean \pm SD. *p<0.05; **p<0.01; ***p<0.001 by Student's 2-tailed t-test or ANOVA.

Impairment of ATP synthesis induces the phosphorylation of MLKL in the activation of necroptosis during lung injury by lung inflammation

We investigated whether the elevated RIPK3 by impaired ATP synthesis could induce the activation of necroptosis in alveolar epithelial cells during lung injury by lung inflammation. We analyzed the levels of MLKL phosphorylation in lung epithelial cells of lung tissues from mice treated with oligomycin during LPS-induced lung inflammation using immunofluorescence staining (**Fig. 3A**, **Supplementary Fig. 1**). The intensity of MLKL phosphorylation (Ser354)-positive staining was significantly elevated in E-cadherin-positive epithelial cells by of Oligomycin + LPS in lung tissues relative to that in LPS (**Fig. 3A and B**). Moreover, the number of epithelial cells with positive subcellular co-localization between MLKL phosphorylation and E-cadherin was significantly higher in Oligomycin + LPS than that in LPS (**Fig. 3C**). Similarly, the levels of RIPK3 and RIPK3 phosphorylation (Thr231/Ser232) were increased by Oligomycin + LPS compared to that in LPS (**Fig. 3D**). The levels of MLKL phosphorylation (Ser345) were increased by Oligomycin + LPS compared to that in LPS (**Fig. 3D**). Furthermore, we analyzed the levels of protein in BALF of mice as a parameter of DAMPs release by the activation of necroptosis (**Fig. 3E**). Consistent with the levels of MLKL phosphorylation, the protein levels of BALF were significantly increased by Oligomycin + LPS compared to relative to that in mice with LPS (**Fig. 3E**). Although the number of inflammatory cells was elevated by LPS relative to that in Control, Oligomycin + LPS did not change the number of inflammatory cells in BALF relative to LPS (**Fig. 3F**). These results suggest that the impairment of ATP synthesis induces the phosphorylation of MLKL in the activation of necroptosis during lung injury by lung inflammation.

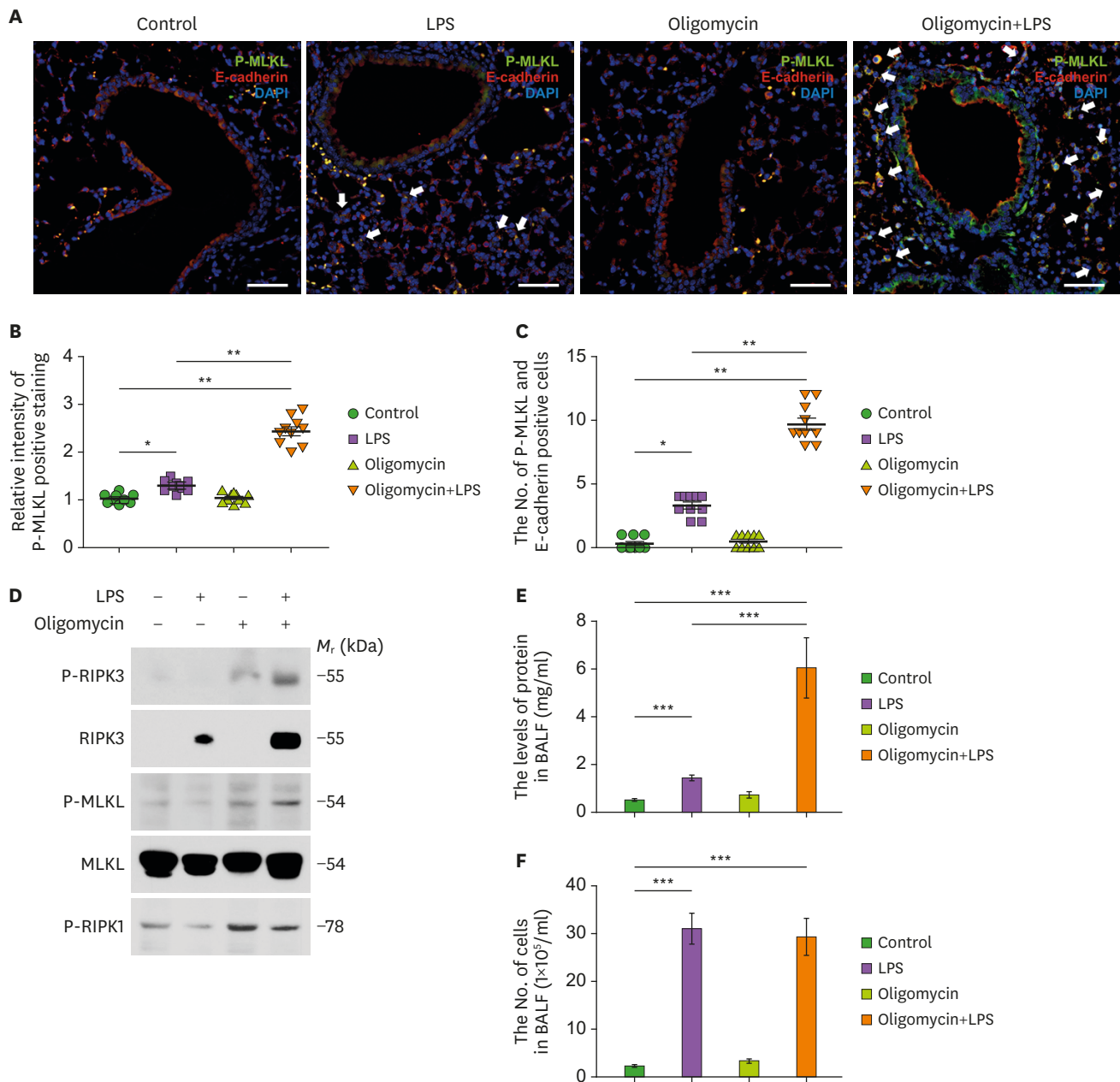


Figure 3. Impairment of ATP synthesis induces the phosphorylation of MLKL in the activation of necroptosis during lung injury by lung inflammation. (A) Representative immunofluorescence images for MLKL phosphorylation at Ser345 (P-MLKL) staining (green) in lung epithelial cells expressing E-cadherin (red) of mice treated with oligomycin either control or LPS. Scale bars, 20 μ m. DAPI-stained nuclei are shown in blue. White arrows indicate P-MLKL positive cells (n=10 images per individual subject, n=5 per each group). (B) Quantification of intensity for P-MLKL-positive staining and (C) quantification of P-MLKL and E-cadherin-positive cells from immunofluorescence images in A. (D) Representative immunoblot images of RIPK3 phosphorylation (Thr231/Ser232), RIPK3, MLKL phosphorylation (Ser345), MLKL, RIPK1 phosphorylation (Ser166) protein from lung tissue sections of A. MLKL was used as loading control. (E) Quantification of protein levels in BALF of lungs from mice treated with oligomycin either control or LPS (n=5 per each group). (F) Quantification of total inflammatory cells in BALF of lungs from mice treated with oligomycin either control or LPS (n=5 per each group). Data are representative of three independent experiments. Data are mean \pm SD. *p<0.05; **p<0.01; ***p<0.001 by Student's 2-tailed t-test or ANOVA.

The reduced ATP5A levels in lung epithelial cells contribute to lung injury of patients with ALI

Next, we investigated whether the impairment of ATP synthesis could contribute to lung injury via the activation of necroptosis during lung injury of patients with ALI. First, we measured the

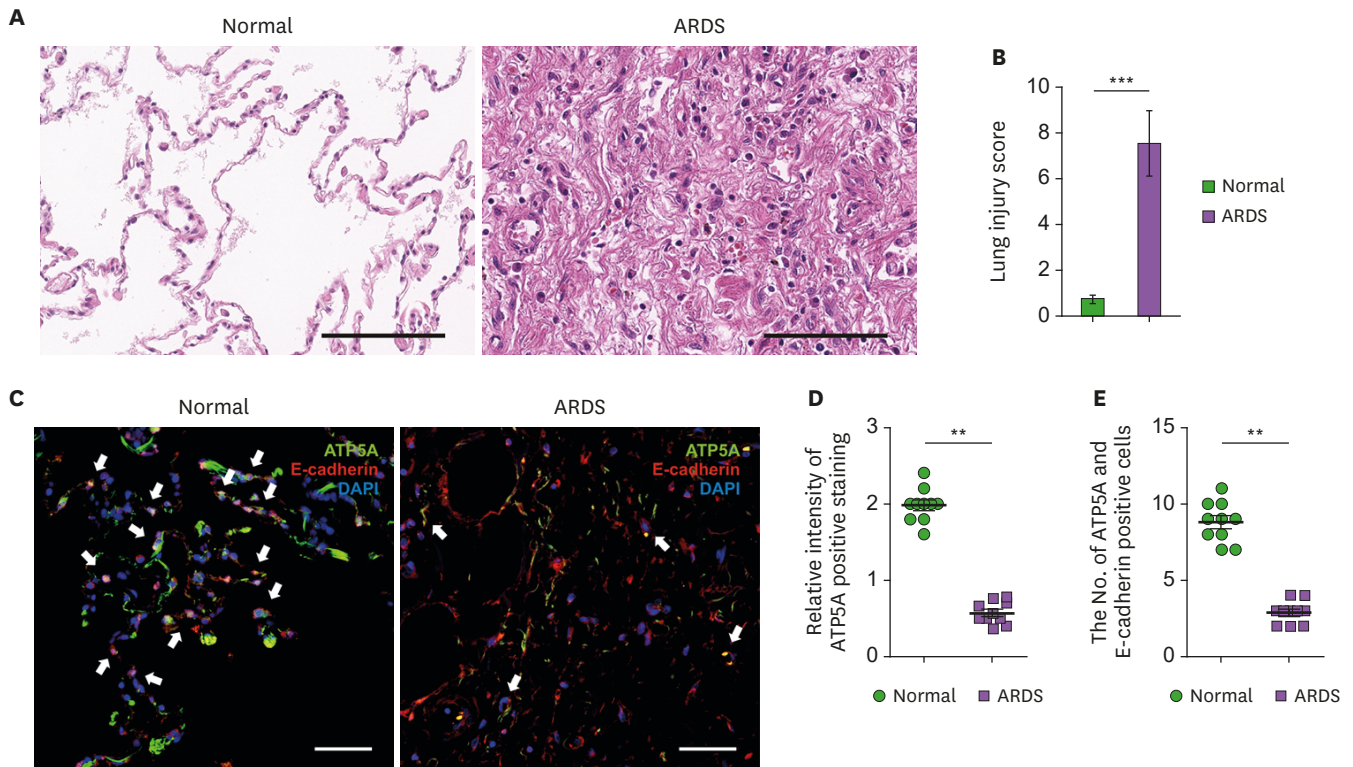


Figure 4. The reduced ATP5A levels in lung epithelial cells contribute to lung injury of patients with ALI. (A) Representative images for H&E staining and (B) quantification of lung injury scores of lung tissues from patients with ARDS (ARDS) and non-ARDS subjects (Normal). Scale bars, 100 μ m. (C) Representative immunofluorescence images for ATP5A staining (green) in lung epithelial cells expressing E-cadherin (red) of ARDS and Normal. Scale bars, 20 μ m. DAPI-stained nuclei are shown in blue. White arrows indicate ATP5A and E-cadherin positive cells. (D) Quantification of intensity for ATP5A-positive staining and (E) quantification of ATP5A and E-cadherin-positive cells from immunofluorescence images in A. Data are representative of three independent experiments. (ARDS, n=7; Normal, n=2; n = 10 images per individual subject). Data are mean \pm SD. **p<0.01; ***p<0.001 by Student's 2-tailed t-test or Mann-Whitney test.

levels of lung injury in lung tissues of patients with ARDS (ARDS), which is the most severe form of ALI, using histopathological analysis. The levels of lung injury, including the hyperplasia of type II pneumocyte, diffuse alveolar damage, and interstitial fibrosis, were elevated in tissues of ARDS compared to that in non-ARDS subjects (Normal) (Fig. 4A and B). Since the production of mitochondrial ATP is regulated by the levels of ATP synthase complex, we analyzed the protein levels of ATP5A, a catalytic subunit of the mitochondrial ATP synthase complex, in lung epithelial cells of lung tissues from patients with ARDS (Fig. 4C, Supplementary Fig. 2). The intensity of ATP5A-positive staining was significantly reduced in E-cadherin-positive epithelial cells of ARDS compared to that in Normal (Fig. 4C and D). Moreover, the number of epithelial cells with positive subcellular co-localization between ATP5A and E-cadherin was significantly decreased in ARDS compared to that in Normal (Fig. 4E). These results suggest that the reduced ATP5A levels in lung epithelial cells contribute to lung injury of patients with ALI.

The levels of RIPK3 are elevated in lung epithelial cells of patients with ARDS

Next, we investigated whether the reduced ATP5A levels could contribute to the elevation of RIPK3 during lung injury of patients with ARDS. We analyzed the protein levels of RIPK3 in lung tissues of patients with ARDS. The intensity of RIPK3-positive staining was elevated in cells of lung tissues from ARDS compared to that in Normal (Fig. 5A and B). Moreover, the number of RIPK3-positive cells was significantly increased in ARDS relative to that in Normal (Fig. 5C). As well as the immunohistochemistry analysis of RIPK3, the levels of RIPK3 were

significantly elevated in lung tissues from ARDS compared to that in Normal (**Fig. 5D**). Consistently, the levels of RIPK3 phosphorylation (Ser227) and MLKL phosphorylation (Ser358) were elevated in lung tissues from ARDS compared to that in Normal (**Fig. 5D**). The levels of RIPK1 phosphorylation (Ser166) were comparable between ARDS and Normal (**Fig. 5D**). These results suggest that the levels of RIPK3 are elevated in lung epithelial cells of patients with ARDS.

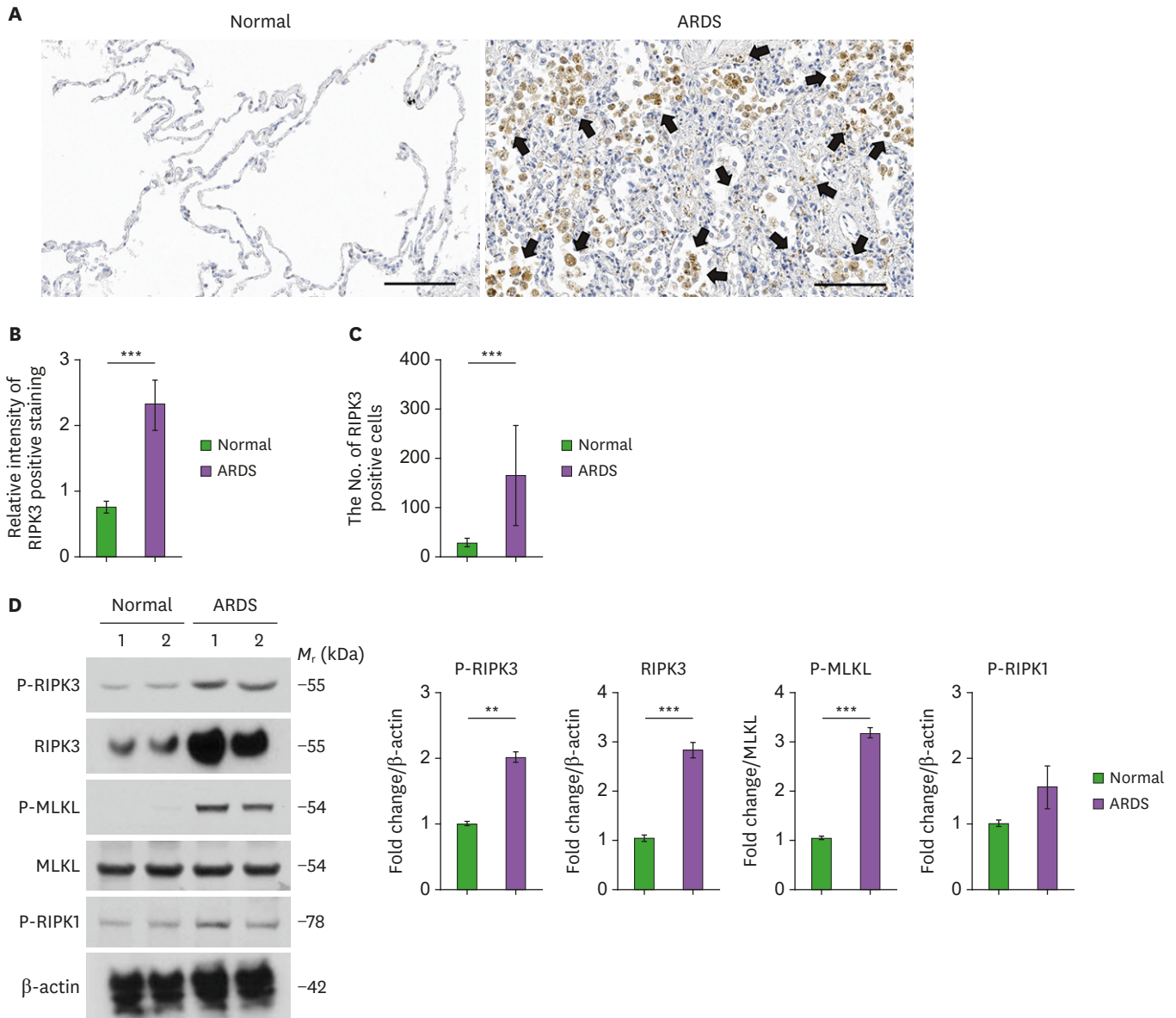


Figure 5. The levels of RIPK3 are elevated in lung epithelial cells of patients with ARDS.

(A) Representative immunohistochemistry images for RIPK3 staining in lung tissues from patients with ARDS (ARDS) and non-ARDS subjects (Normal). Scale bars, 100 μm. Black arrows indicate RIPK3-positive cells. (B) Quantification of intensity for RIPK3-positive staining in cells and (C) quantification of RIPK3-positive cells from immunohistochemistry images in A (ARDS, n=7; Normal, n=2; n = 10 images per individual subject). (D) Representative immunoblot images of RIPK3 phosphorylation (Ser227), RIPK3, MLKL phosphorylation (Ser358), MLKL, RIPK1 phosphorylation (Ser166) protein levels (left) and quantification of RIPK3 phosphorylation, RIPK3, MLKL phosphorylation, RIPK1 phosphorylation protein levels (right) in lung tissues from ARDS and Normal (n=2 per each group). β-actin or MLKL were used as loading control. Data are representative of three independent experiments. Data are mean±SD. **p<0.01; ***p<0.001 by Student's 2-tailed t-test or Mann-Whitney test.

The activation of necroptosis by MLKL phosphorylation is elevated in lung epithelial cells of patients with ARDS

Next, we investigated whether the high levels of RIPK3 could promote the activation of necroptosis by MLKL phosphorylation in lung epithelial cells of patients with ARDS. We analyzed the levels of MLKL phosphorylation in lung epithelial cells of patients with ARDS using immunofluorescence staining (Fig. 6A, Supplementary Fig. 3). The intensity of MLKL phosphorylation (Ser358)-positive staining was significantly elevated in E-cadherin-positive epithelial cells in lung tissues of ARDS relative to that in Normal (Fig. 6A and B). Moreover, the number of epithelial cells with positive subcellular co-localization between MLKL phosphorylation and E-cadherin was significantly increased in ARDS relative to that in Normal (Fig. 6C). Similarly, the levels of RIPK3 and RIPK3 phosphorylation (Ser227) were increased in ARDS relative to that in Normal (Fig. 6D). The levels of MLKL phosphorylation (Ser358) were increased in ARDS relative to that in Normal (Fig. 6D). In summary, our results suggest that the impaired mitochondrial ATP synthesis induces RIPK3-dependent necroptosis in lung epithelial cells during lung injury by lung inflammation (Fig. 6E).

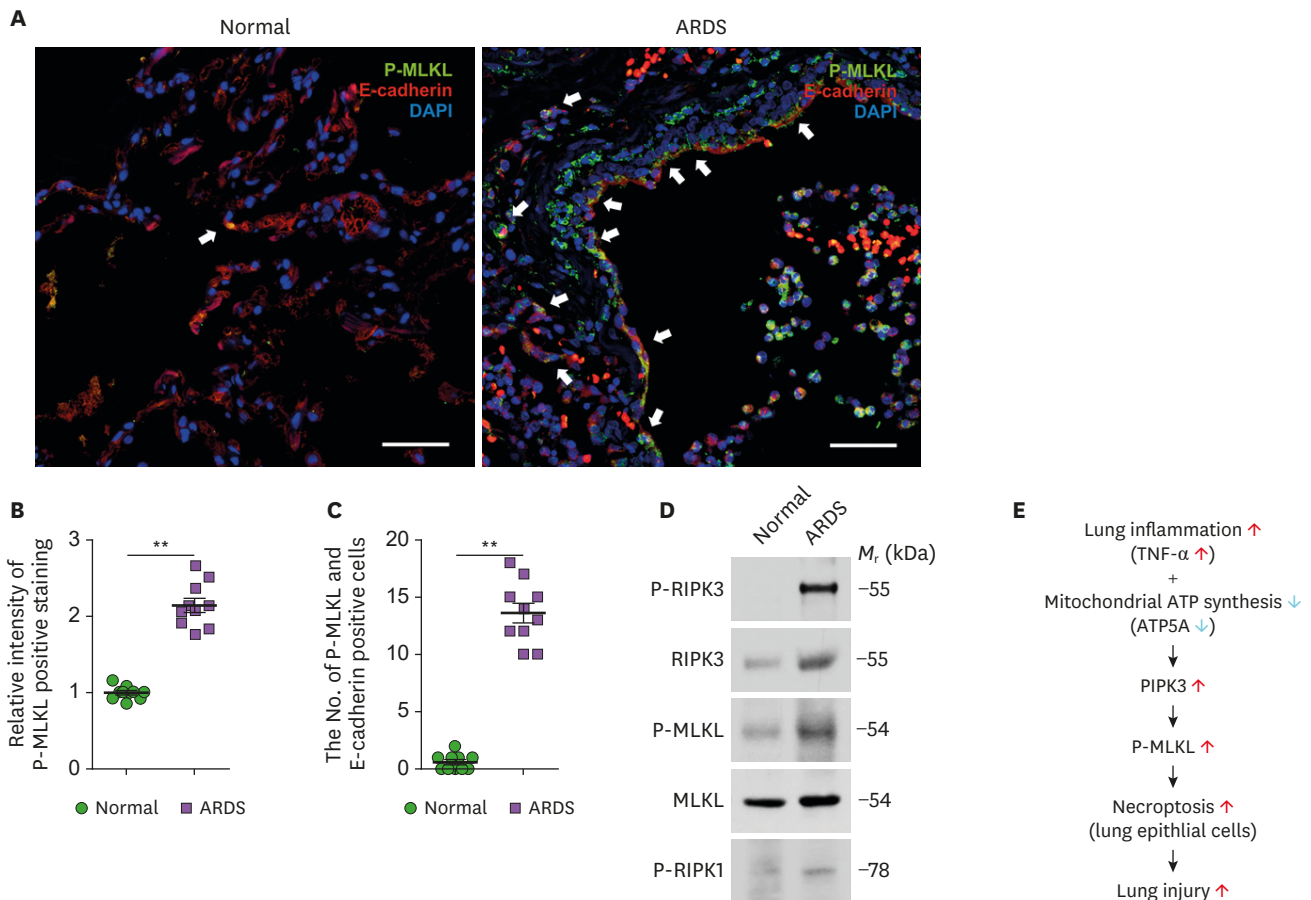


Figure 6. The activation of necroptosis by MLKL phosphorylation is elevated in lung epithelial cells of patients with ARDS. (A) Representative immunofluorescence images for MLKL phosphorylation at Ser358 (P-MLKL) staining (green) in lung epithelial cells expressing E-cadherin (red) of lung tissues from patients with ARDS (ARDS) and non-ARDS subjects (Normal). Scale bars, 20 μm. DAPI-stained nuclei are shown in blue. (B) Quantification of intensity for P-MLKL-positive staining and (C) quantification of P-MLKL and E-cadherin-positive cells from immunofluorescence images in A (ARDS, n=7; Normal, n=2; n=10 images per individual subject). (D) Representative immunoblot images of RIPK3 phosphorylation (Ser227), RIPK3, MLKL phosphorylation (Ser358), MLKL, RIPK1 phosphorylation (Ser166) protein from lung tissue sections of A. MLKL was used as loading control. (E) A schematic diagram to summarize our new findings. Red arrow means an increase and blue arrow means a decrease in the diagram. Data are representative of 3 independent experiments. Data are mean ± SD. **p<0.01 by Student's 2-tailed t-test.

DISCUSSION

In this study, we demonstrate that the impaired mitochondrial ATP synthesis induces RIPK3-dependent necroptosis in lung epithelial cells during lung injury by lung inflammation. Our results showed that the impairment of ATP synthesis promotes RIPK3-dependent necroptosis via MLKL phosphorylation in lung epithelial cells during inflammation. Also, we showed that the reduction of ATP5A levels contributes to the activation of necroptosis by RIPK3-MLKL phosphorylation in lung epithelial cells of patients with ARDS.

ALI is a clinical syndrome characterized by an acute inflammatory process in the lung tissue and airways (17). Acute inflammation leads to the loss of barrier function of the lung epithelial cells and pulmonary capillary endothelial cells (18). Oxidative stress is associated with the pathological processes in ALI (19). Oxidative stress is characterized by the over-production of ROS, damage of mitochondrial respiratory chain, changes of membrane permeability, and imbalance of Ca^{2+} homeostasis and mitochondrial defense systems (20). Our results suggest that the impairment of ATP synthesis could be a critical for the mitochondrial dysfunction in lung epithelial cells during lung injury by lung inflammation. Also, our findings suggest that the activation of RIPK3-dependent necroptosis via MLKL phosphorylation might be a critical cell death pathway under mitochondrial dysfunction in lung injury by lung inflammation.

As the most severe form of ALI, the initial pathogenesis of ARDS is related to the damage and death of alveolar endothelial cells and epithelial barrier cells (21). A previous study showed that apoptosis is linked to the cell death of epithelial cells during ARDS (22). Additionally, necroptotic cell death contributes to the lung injury in ARDS (23,24). The plasma levels of RIPK3 were increased in patients with ARDS (23). Consistent with previous study, our results showed that the activation of RIPK3-dependent necroptosis via MLKL phosphorylation was elevated in lung epithelial cells of patients with ARDS. While our study showed the impairment of ATP synthesis induces the activation of necroptosis in lung epithelial cells during lung injury by lung inflammation, further study for the effects of mitochondrial dysfunction in lung endothelial cells in the regulation of necroptosis during lung inflammation is needed.

Conclusively, our results suggest that the impairment of ATP synthesis might be a critical for necroptotic cell death during lung injury by lung inflammation.

ACKNOWLEDGEMENTS

This work was funded by the National Research Foundation of Korea (NRF) grant funded by the Korea government (MSIT) (NRF-2018R1C1B6004282 to Su Hwan Lee) and National Research Foundation of Korea (NRF-2021R1C1C1007810 and NRF-2019M3E5D1A02069071 to Jong-Seok Moon) and Soonchunhyang University Research Fund to Jong-Seok Moon.

SUPPLEMENTARY MATERIALS

Supplementary Table 1

Baseline characteristic of in enrolled subjects

[Click here to view](#)

Supplementary Table 2

Lung injury score parameters

[Click here to view](#)

Supplementary Figure 1

The levels of MLKL phosphorylation were elevated in lung epithelial cells of lung tissues from mice treated with oligomycin either control or LPS. Representative immunofluorescence images of MLKL phosphorylation (Ser358) levels in lung tissues from mice treated with oligomycin either control or LPS showing MLKL phosphorylation at Ser358 (P-MLKL, green) in lung epithelial cells expressing the epithelial cells marker E-cadherin (red). DAPI-stained nuclei are shown in blue. Scale bars, 20 μ M. White arrows indicates MLKL phosphorylation (Ser358) and E-cadherin positive cells.

[Click here to view](#)

Supplementary Figure 2

The levels of ATP5A were reduced in lung epithelial cells of lung tissues from patients with ARDS. Representative immunofluorescence images of ATP5A expression in lung tissues from patients with ARDS (ARDS) or non-ARDS subjects (Normal) showing ATP5A (green) in lung epithelial cells expressing the epithelial cells marker E-cadherin (red). DAPI-stained nuclei are shown in blue. Scale bars, 20 μ M. White arrows indicates ATP5A and E-cadherin positive cells.

[Click here to view](#)

Supplementary Figure 3

The levels of MLKL phosphorylation were elevated in lung epithelial cells of lung tissues from patients with ARDS. Representative immunofluorescence images of MLKL phosphorylation (Ser358) levels in lung tissues from patients with ARDS (ARDS) or non-ARDS subjects (Normal) showing MLKL phosphorylation at Ser358 (P-MLKL, green) in lung epithelial cells expressing the epithelial cell marker E-cadherin (red). DAPI-stained nuclei are shown in blue. Scale bars, 20 μ M. White arrows indicates MLKL phosphorylation (Ser358) and E-cadherin positive cells.

[Click here to view](#)

REFERENCES

1. Schumacker PT, Gillespie MN, Nakahira K, Choi AM, Crouser ED, Piantadosi CA, Bhattacharya J. Mitochondria in lung biology and pathology: more than just a powerhouse. *Am J Physiol Lung Cell Mol Physiol* 2014;306:L962-L974.
[PUBMED](#) | [CROSSREF](#)
2. Martínez-Reyes I, Cuezva JM. The H(+)-ATP synthase: a gate to ROS-mediated cell death or cell survival. *Biochim Biophys Acta* 2014;1837:1099-1112.
[PUBMED](#) | [CROSSREF](#)
3. Sena LA, Chandel NS. Physiological roles of mitochondrial reactive oxygen species. *Mol Cell* 2012;48:158-167.
[PUBMED](#) | [CROSSREF](#)

4. Bhatia M, Zemans RL, Jeyaseelan S. Role of chemokines in the pathogenesis of acute lung injury. *Am J Respir Cell Mol Biol* 2012;46:566-572.
[PUBMED](#) | [CROSSREF](#)
5. Matthay MA, Zemans RL. The acute respiratory distress syndrome: pathogenesis and treatment. *Annu Rev Pathol* 2011;6:147-163.
[PUBMED](#) | [CROSSREF](#)
6. Martin TR, Hagimoto N, Nakamura M, Matute-Bello G. Apoptosis and epithelial injury in the lungs. *Proc Am Thorac Soc* 2005;2:214-220.
[PUBMED](#) | [CROSSREF](#)
7. Schurr JR, Young E, Byrne P, Steele C, Shellito JE, Kolls JK. Central role of Toll-like receptor 4 signaling and host defense in experimental pneumonia caused by gram-negative bacteria. *Infect Immun* 2005;73:532-545.
[PUBMED](#) | [CROSSREF](#)
8. Branger J, Knapp S, Weijer S, Leemans JC, Pater JM, Speelman P, Florquin S, van der Poll T. Role of Toll-like receptor 4 in gram-positive and gram-negative pneumonia in mice. *Infect Immun* 2004;72:788-794.
[PUBMED](#) | [CROSSREF](#)
9. Patel BV, Wilson MR, O'Dea KP, Takata M. TNF-induced death signaling triggers alveolar epithelial dysfunction in acute lung injury. *J Immunol* 2013;190:4274-4282.
[PUBMED](#) | [CROSSREF](#)
10. Matthay MA, Zemans RL, Zimmerman GA, Arabi YM, Beitler JR, Mercat A, Herridge M, Randolph AG, Calfee CS. Acute respiratory distress syndrome. *Nat Rev Dis Primers* 2019;5:18.
[PUBMED](#) | [CROSSREF](#)
11. Galluzzi L, Vanden Berghe T, Vanlangenakker N, Buettner S, Eisenberg T, Vandenabeele P, Madeo F, Kroemer G. Programmed necrosis from molecules to health and disease. *Int Rev Cell Mol Biol* 2011;289:1-35.
[PUBMED](#) | [CROSSREF](#)
12. Feoktistova M, Leverkus M. Programmed necrosis and necroptosis signalling. *FEBS J* 2015;282:19-31.
[PUBMED](#) | [CROSSREF](#)
13. Kaczmarek A, Vandenabeele P, Krysko DV. Necroptosis: the release of damage-associated molecular patterns and its physiological relevance. *Immunity* 2013;38:209-223.
[PUBMED](#) | [CROSSREF](#)
14. Rodriguez DA, Weinlich R, Brown S, Guy C, Fitzgerald P, Dillon CP, Oberst A, Quarato G, Low J, Cripps JG, et al. Characterization of RIPK3-mediated phosphorylation of the activation loop of MLKL during necroptosis. *Cell Death Differ* 2016;23:76-88.
[PUBMED](#) | [CROSSREF](#)
15. Koo MJ, Rooney KT, Choi ME, Ryter SW, Choi AM, Moon JS. Impaired oxidative phosphorylation regulates necroptosis in human lung epithelial cells. *Biochem Biophys Res Commun* 2015;464:875-880.
[PUBMED](#) | [CROSSREF](#)
16. Matute-Bello G, Downey G, Moore BB, Groshong SD, Matthay MA, Slutsky AS, Kuebler WM; Acute Lung Injury in Animals Study Group. An official American Thoracic Society workshop report: features and measurements of experimental acute lung injury in animals. *Am J Respir Cell Mol Biol* 2011;44:725-738.
[PUBMED](#) | [CROSSREF](#)
17. Ware LB, Matthay MA. The acute respiratory distress syndrome. *N Engl J Med* 2000;342:1334-1349.
[PUBMED](#) | [CROSSREF](#)
18. Ware LB. Pathophysiology of acute lung injury and the acute respiratory distress syndrome. *Semin Respir Crit Care Med* 2006;27:337-349.
[PUBMED](#) | [CROSSREF](#)
19. Chow CW, Herrera Abreu MT, Suzuki T, Downey GP. Oxidative stress and acute lung injury. *Am J Respir Cell Mol Biol* 2003;29:427-431.
[PUBMED](#) | [CROSSREF](#)
20. Bhatti JS, Bhatti GK, Reddy PH. Mitochondrial dysfunction and oxidative stress in metabolic disorders - a step towards mitochondria based therapeutic strategies. *Biochim Biophys Acta Mol Basis Dis* 2017;1863:1066-1077.
[PUBMED](#) | [CROSSREF](#)
21. Thompson BT, Chambers RC, Liu KD. Acute respiratory distress syndrome. *N Engl J Med* 2017;377:562-572.
[PUBMED](#) | [CROSSREF](#)
22. Galani V, Tatsaki E, Bai M, Kitsoulis P, Lekka M, Nakos G, Kanavaros P. The role of apoptosis in the pathophysiology of acute respiratory distress syndrome (ARDS): an up-to-date cell-specific review. *Pathol Res Pract* 2010;206:145-150.
[PUBMED](#) | [CROSSREF](#)

23. Shashaty MGS, Reilly JP, Faust HE, Forker CM, Ittner CAG, Zhang PX, Hotz MJ, Fitzgerald D, Yang W, Anderson BJ, et al. Plasma receptor interacting protein kinase-3 levels are associated with acute respiratory distress syndrome in sepsis and trauma: a cohort study. *Crit Care* 2019;23:235.
[PUBMED](#) | [CROSSREF](#)
24. Faust H, Mangalmurti NS. Collateral damage: necroptosis in the development of lung injury. *Am J Physiol Lung Cell Mol Physiol* 2020;318:L215-L225.
[PUBMED](#) | [CROSSREF](#)